K. Prabu[1,*],
J. Srinivasan[2],
C. Prakash[3]

Ceramic and Glass Fibre Reinforced Flexible Composites for Particulate Filter Walls – A Novel Approach

DOI: 10.5604/01.3001.0012.7747

[1] Department of Fashion Technology,
Kumaraguru College of Technology,
Coimbatore 641049, India
* Corresponding author
e-mail: prabukrishnaa@yahoo.com

[2] Department of Textile Technology,
Kumaraguru College of Technology,
Coimbatore 641049, India

[3] Department of Fashion Technology,
Sona College of Technology,
Salem-636005, Tamil Nadu India

Abstract
Flexible composites from high performance fibres were developed and targeted to replace the wall of existing rigid ceramic Particulate Filters. The composites are made from E Glass fibre webs of different density in the middle, with standard SiC Ceramic fibres webs in in the outer layers, forming a sandwich structure. Different needling densities were applied to form nonwoven composites, and they were stitched diagonally on the surface at specified intervals with continuous glass fibre filament yarn. In total, nine novel flexible composites were developed and evaluated for their structural, surface, mechanical and thermal properties. Based on the results and statistical analysis, the B2 sample is considered to be taken for further research to develop Particulate Matter (PM) filters.

Key words: *PM – particulate matters, SiC – silicon carbide.*

Introduction

There is increasing usage of diesel engine vehicles since they have greater energy density when compared with petrol of the same volume, and they show a 10-20% reduction in CO_2 exhaust [1]. However, diesel engines are among the major air polluters, not only in the quality of emission but also regarding the particulate matters (PM). Emission standards are continuously more restrictive, particularly for diesel engines. There are several technologies available for exhaust treatments such as the application of catalytic convertors with imparting oxidation techniques. However, the PMs emitted are a major constituent of air pollution. The size ranges from 2.5 to 10 microns, which causes respiratory problems, skin cell alterations as well as cardiovascular diseases [2]. An efficient solution in the field of PM reduction and filtration in diesel engines is a complex and dynamic system called diesel particulate filters (DPF).

DPFs are made of extruded cordierite or silicon carbide ceramic with a cylindrical filter of a cross-section in a honeycomb structure. Of the various filters, the wall-flow structures are more efficient in their performances [3]. The wall thickness of one layer is 0.38 mm [4]. With a wall-flow filter; the exhaust is passed through fine porous ceramic walls which have a filtration rate of over 90%. However, an efficient regeneration process is required in a wide range of engines to prevent clogging, which results in the formation of backpressure in the exhaust, leading to higher consumption of fuel and, in the worst case, damage to the engine and filter [5].

Owing to other high performance materials of lower cost, alternative flexible composite materials are examined to analyse the filtration performance of particulate matters, aiming at increasing filtration performance along with thermal stability to support filtration. In this research work, nonwoven fibrous flexible composite material was developed using ceramic and glass fibres. It was optimised based on characterisation analysis of the fibrous composites for their surface, mechanical and thermal properties.

A new approach was taken for the fibrous composites where the flow length of air passing through the media was higher than the for the rigid filter of existing media. These phenomena may result in a reduction in the bouncing/back flow of air after collision with the rigid wall. For typical diesel exhausts from engines, the temperature falls between 200-500 °C [6, 7], and a material was proposed to be placed in the catalytic converter after catalysis taking place, where the temperature ranges between 300-550 °C [1].

Although existing particulate filters are with a fine wall thickness of approximately of 0.38 mm [4] and with a rigid cylindrical surface of multiple walls arranged in a honeycomb structure, this paper deals with a single flexible wall developed and selected by considering the filter wall properties expected. These flexible walls achieved 10% of their mechanical properties in the data tested compared to existing DPF properties [4]. The media developed is to be used with a proper gridded design of the filtration assembly to adopt flexible walls.

Table 1. *General properties of the constitutive materials.*

Properties	E Glass fibre	Ceramic fibre (SiC)
Temperature rating, °C	800	1260
Density, g/m^3	2.58	3.21
Specific gravity, g/m^3	2.54	2.7
Diameter, μm	12-18	2-6
No. of filament structures	Multifilament (32)	Mono short fibres
Thermal expansion 10^{-6}/K	4.9-5.1	4.7-5.2

Materials and methods

Existing DPFs consist of channels with a honeycomb structure, allowing flow through the channels and providing a more specific area [3]. Based on this phenomenon, the middle layer of the flexible composite is applied with a spacious

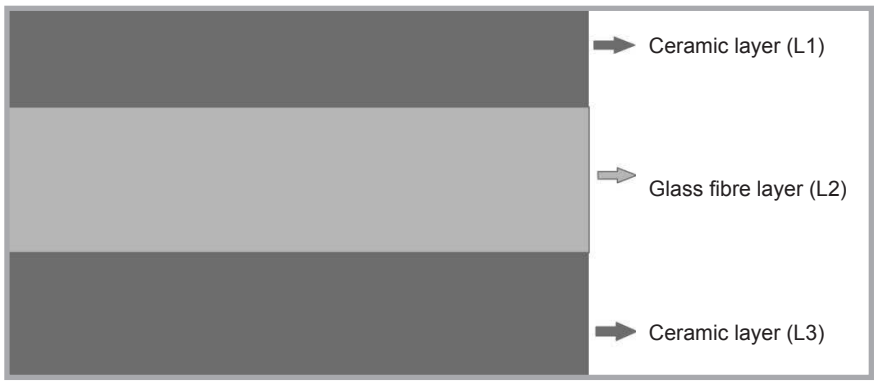

Figure 1. *Specimen constructed with ceramic web - glass fibre web - ceramic web.*

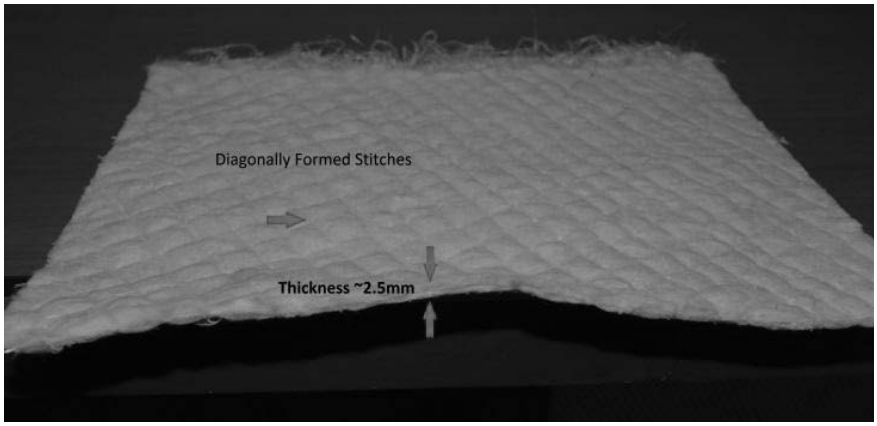

Figure 2. *Finished sample after needle punching and diagonal stitching with glass filament yarn.*

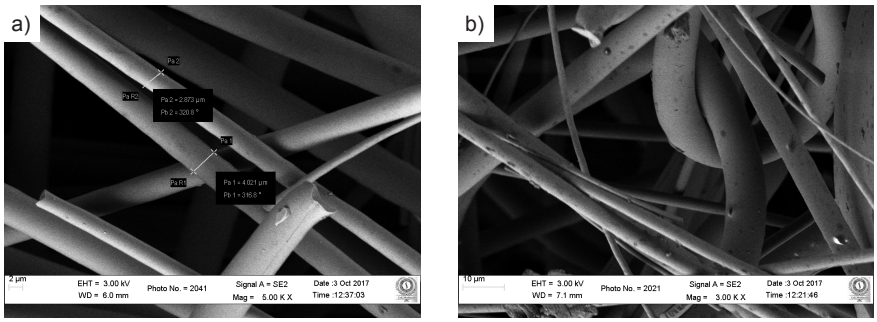

Figure 3. *a) Microstructure of ceramic fibres, b) interlocking of fibres by needle punching.*

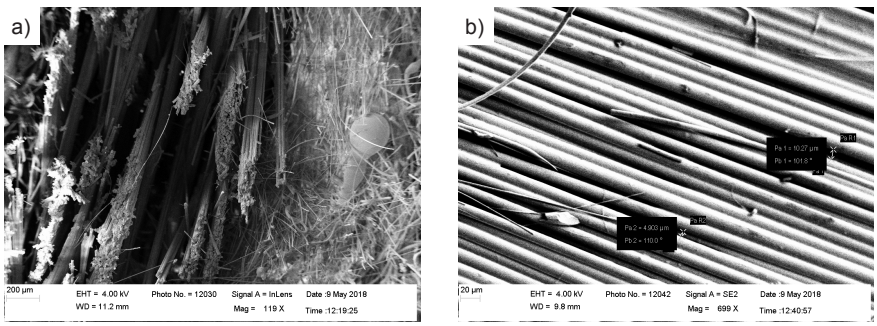

Figure 4. *a) Cross sectional view of glass fibre arrangement between the ceramic layer, b) Micro fibril arrangement of the glass fibre and space between fibrils.*

structured glass fibre web with a coarse fibre type nonwoven layer of different thickness. Moreover the glass fibres have a fibril structure with various sizes of microns ranging from 10.0 to 18.0 µm, arranged together, which provides trapping space for particles. The basic properties of the selection of raw materials for the research were taken as per the data given in ***Table 1***.

Preparation of flexible composites

The composite materials were prepared as three-layer nonwoven web samples. The constitutive web layers were arranged in such a way to create a Ceramic-Glass fibre – Ceramic layer (CGC), with a SiC ceramic web of 3.0 mm thickness, combined with a glass fibre web of three different material weight combinations, such as 250, 300 and 350 g/m^2, with an average thickness of 0.39, 0.55 and 0.70 mm, respectively. The layers are arranged in such a manner that there are ceramic (SiC) webs in the outer layers and the middle layer is of glass fibre, a schematic diagram is shown in ***Figure 1***. The composites are needle punched using different needling densities i.e. 75, 100 and 125 punches/cm^2, a total of 9 different flexible composite samples were prepared and coded as samples A1-A3, B1-B3 and C1-C3, as shown in ***Table 2***. The punching was carried out at a speed of 25 strokes (215 Cycles/min) with a 5 mm depth of penetration. The machine used for the needle punching was a Dilo (German), and the process was carried out with a barbed needle of 15×18×36×3.5 R/SP dimensions. The samples were then stitched diagonally with 100 Denier glass filament yarn at 8 stitches per inch, having an interval of 10 mm distance between the stitch lines to improve tensile performance; the final sample is shown in ***Figure 2***. This process will enable a compressed flexible nonwoven composite structure with improved strength. This phenomenon is to prepare a wall similar to regular DPF walls only by varying the thickness in a higher range.

Structural – properties of the composite materials

Randomised fibre arrangement layered webs are used in both materials. The ceramic fibres and E-Glass fibres used range from 2.8 to 4.0 µm. The interlocking of fibres by needle punching is shown in ***Figure 3*** in SEM images. Subsequently the glass fibres are further separated into fibrils of 12 to 18 µm, with spaces between them ranging from 4.9 to 10.27 µm, which aids porosity as well as trapping particles. a cross sectional view of the glass fibres between ceramic fibres is shown in ***Figure 4*** in SEM images.

As a flexible composite was planne, for the DPF walls, the major property requirement for the component is minimum thickness with higher pore sizes, air permeability, and a high density surface to capture particle matter. However, the thermal properties also play an important role in selecting the filter walls inside the exhaust system; materials with higher thermal conductivity can conduct certain heat for the reproduction process to burn unburnt soot particles. Mechanical behavior such as high tensile and bursting strength are expected to be good; consequently, the walls can withstand the continuous flow of exhaust pressure applied from multiple directions [3].

Testing methods

Thickness test

The thickness of the layers of ceramic and glass fibre was tested after needle punching with different needling densities: 75, 100 and 125 punches/cm^2. The difference in the thickness due to the change in needling density was measured using a Shirley thickness guage according to the ASTM D1777-96 (2015) standard [8].

Porosity

The irregular structure of nonwoven shows difficult characterisation of porosity, which make them more effective and efficient media for filtration [9], playing a major role in filtration area. In the application of ceramic and glass fibre nonwoven composites with different densities, no reliable porosity can be measured by an image analysis technique because of the higher thickness and the fact that the smallest pores may be closed. Furthermore the distribution of pore sizes will, in a broad manner, make the simultaneous detection of larger and smaller pore sizes difficult [3]. Pore sizes were examined and characterised using a porometer as instructed in ASTM E1294-89.

Air permeability

The air permeability of the samples were determined by the rate of air flow passing perpendicularly through a set area under given pressure over a given time period. The air permeability properties of the fabrics were measured using Atlas air permeability instrument according to BS 5636 [10] standard with 100 Pa air pressure. It is expressed as the quantity of air in cubic centimeter passing per second through a square centimeter of fabric.

Table 2. *Design of sample.*

Ceramic web, g/m^2	E Glass web, g/m^2	Needling density, punches/cm^2	Sample code
200	250	75	A1
		100	A2
		125	A3
	300	75	B1
		100	B2
		125	B3
	350	75	C1
		100	C2
		125	C3

Tensile strength

Though the samples evolve under air pressure, its minimal requirement of tensile force where the bursting strength is mandatory to analyse. The non-woven undergoes the stitch process to increase its strength, and tensile analysis is conducted multidirectional though the fibres are arranged in multidirectional. Testing of the tensile force in N and elongation is undertaken with a Uni stretch machine according to the ASTM D 5035 [11] standard, at a rate of elongation of 300 mm/min and pretension of 1 gram.

Bursting strength

As the randomised fibre arrangement in the needle punched nonwoven and air passage through the wall of the filtration media are multidirectional, the specimen is evaluated for its bursting strength. The specimen is held by clamps and subjected to pressure hydraulically through an expanding diaphragm. The Bursting strength is examined using an MAG AutoBurst 28, with a 100 mm dial, 1.2" diameter hole, and test specimen size of 125 × 125 mm, following the ASTM D3786 method [12].

Thermal properties

Regarding thermal properties, it is more important to analyse them when the material is applied om DPF walls. These walls are designed for inside a catalytic convertor in an exhaust system, where the temperature will be similar to that of light duty diesel engine exhausts with a catalytic converter, as mentioned in [1].

Thermal conductivity measurement

Thermal conductivity (λ) in a steady-state is determined according to ASTM C 518 by the heat flow technique [13], with sample size 30.5 × 30.5 cm, and upper plate temperature of 90 °C and 30 °C on the lower plate. The plate is transportable, hence various thicknesses of composite with different compositions can be tested [14]. Heat transfer occurs by solid/gas conduction as well as thermal radiation mechanisms. The temperature of the plates are controlled by bidirectional peltier systems, a closed-loop, and heating and cooling take place by fluid flow with a forced-air incorporated heat exchanger. Two heat flux temperature transducers help in measuring the values. For the samples, to maintain the allowed time limit of 12-14 min [15], the temperature was measured. The unit of measurement of thermal conductivity – λ is W/(m·K).

$$Q = \lambda A \frac{\Delta T}{L} \text{ W/(m·K)} \qquad (1)$$

Where,

Q – Heat flow rate, W
λ – Thermal conductivity, W/(m·K)
A – Meter area normal to heat flow, m^2
ΔT – Temperature difference across the specimen, K
L – In-situ specimen thickness, m.

Thermal resistivity

Resistivity is normally inversely proportional to conductivity. Standard EN ISO 6946 explains that the thermal resistance of a layered composite can obtained by dividing the thermal conductivity of the non-woven composite by its thickness (T) [16] and by the value of

$$R = T/\lambda, \text{ (m}^2\text{ K)/W} \qquad (2)$$

Thermal transmittance (U)

At a 1 K heat difference between the surfaces in the heat flow directions, the time rate of heat flow through 1 m^2 of the component is termed as the transmittance. U value, which can be calculated for a given composite [17] and is represented in W/(m^2 K)

$$U = 1/R \text{ W/(m2 K)} \qquad (3)$$

***Thermal diffusivity* (α)**

Thermal diffusivity measures the capacity to conduct in proportion to the storage of thermal energy of a composite. It indicates how rapidly a composite can vary the temperature in reaction to to heat [18]. It is denoted usually by α in m^2/s.

$$\alpha = \frac{\lambda}{\rho C_p}, \text{ m2/s} \qquad (4)$$

Where,

λ – Thermal conductivity W/(m K)

ρ – Density (kg/m^3)

C_p – Specific heat capacity J/(kg K).

Results and discussion

Effect of needle punching process on thickness and density

The thickness of the samples initially was 6.39, 6.55 and 6.70 mm for the A, B and C series of samples, respectively. which were standardised in their thickness as well as in their densities. However, the needling densities and the density of the glass fibre layer react to the compression of the final thickness of the material. The finished samples have a compression ranging from a 44.28% reduction in thickness in 75 punches/cm^2 with 250 g/m^2 of glass fibre sample A1 to a maximum compression of 62.83% in sample C2 of 100 punches/cm^2 with 300 g/m^2. ***Figure 5*** shows the compression percentage (reduction in thickness in %) after finishing. From the results, it is concluded that the lower needle density is influenced by the reduction in intermeshing and higher punching rate, where the needle itself opens up the layer, and hence the thickness is not much compressed. ***Figure 5*** shows very well that in all the samples, 100 punches/cm^2 has a good impact on the binding of fibres between layers in intermeshing and reducing the thickness in a compact manner. On the other hand, the fibre content of the glass fibre layer also has an impact on the compression of thickness, where 250 g/m^2 fibres have a lower amount of intermeshing, which influences the thickness, and in the case of the 350 g/m^2 sample C series, greater glass fibre content will open the short fibrous component of the ceramic structure, which again reverses the process of compressing the material, making a more finished thickness.

On the other hand, density due to needle punching increased when the thickness decreased. ***Figure 6*** shows directly the influence of the needling density, where 75 punches/cm^2 makes a lower percentage of the increase in density of the resultant material and vice-versa in each set of samples. Meanwhile the glass fibre content, which is the reason behind the intermeshing of fibres, also influences samples B3 and C3 as well as the higher needle punching of 125 punches/cm^2, causing the opening up of the intermeshed layers during production. Moreover the percentage increase in density is reduced compared to samples B2 and C2, whose densities increase from their initial to a maximum of 1.5 and 1.6 times, respectively.

Effect of needle punching process on strength and elongation properties

Although the nonwoven flexible composite material is made of a multidirectional web alignment, the fibre intermeshing influences both the strength properties of the raw material as well as the punching density.

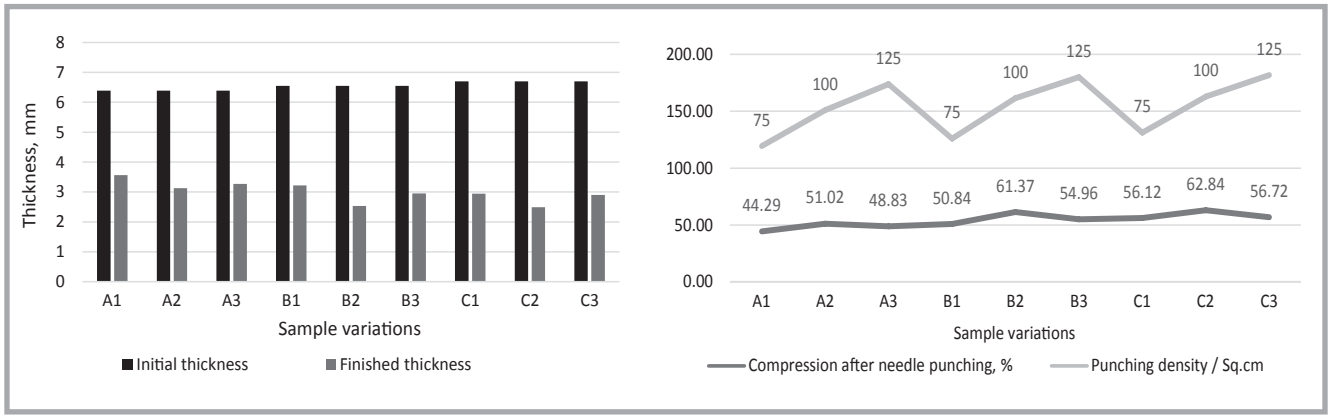

Figure 5. *Effect of needle punching and materials on thickness.*

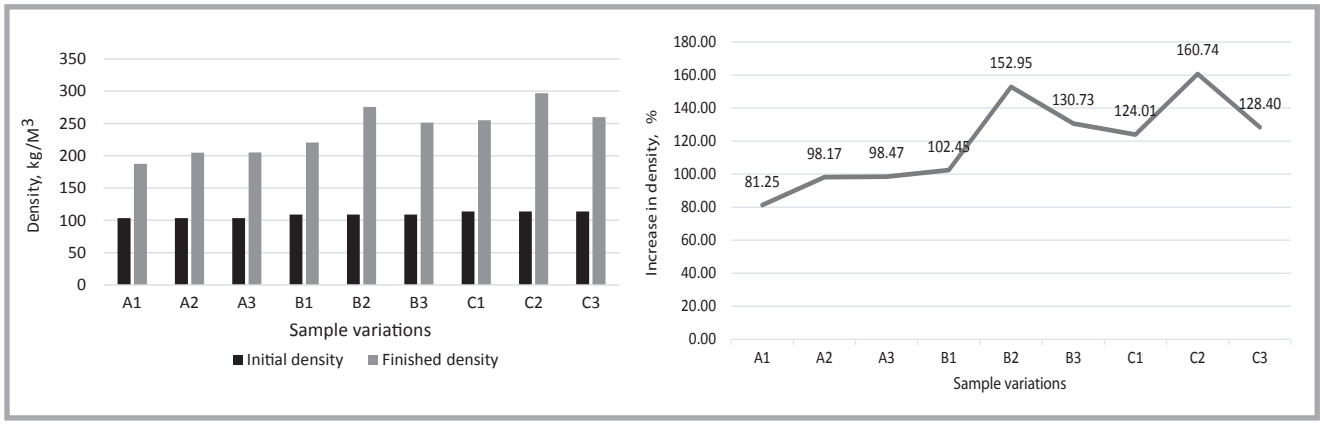

Figure 6. *Effect of needle punching and materials on density.*

Figure 7, clearly shows the tensile, bursting and elongation property peaks of samples A3, B2 and C1, giving average glass fibre/needling densities of 250 g/m^2/125 punches/cm^2, 300 g/m^2/100 punches/cm^2, and 350 g/m^2/125 punches/cm^2, respectively.

This explains that there is a minimum contribution of the ceramic fibre to strength properties as well as the influence is minimal in this combinations.

Effect on mechanical properties

The application of a glass fibre web was made on the basis of improving the mechanical strength of the layer of glass fibre non-woven containing a higher fibre length. When needle punched, the interlocking of the fibre web results in intertwining, which, due to the fibre friction caused between these different layers, improves the strength of the nonwoven filter layer. Consequently the thickness of the ceramic layers is considerably reduced, increasing in the density of the surface.

Physical and mechanical properties such as thickness, density, tensile strength and elongation, as well as the bursting strength of the 9 samples of flexible composites made of ceramic/glass fibre nonwoven webs are given in the ***Table 3***. On average, 15 readings are noted for the thickness and 10 for the other parameters examined for the analysis.

Thickness is a major criterion for filtration media as it influences the density and other morphological parameters, such as porosity and air permeability. C2 and B2 showed a minimal thickness of 2.49 and 2.53 mm with higher densities of 296.70 and 275.50 kg/m^3. Meanwhile, when it comes to the strength of the material, though it is a nonwoven; the multidirectional arrangement of the fibrous surfaces caused a concentration of the bursting strength; although the flow of air through the wall was also multidirectional. B2 shows a higher bursting strength value of 1.25 MPa, and with its higher tensile strength of 55.9 N, B2 is a better option for the wall flow filtration process among the 9 samples. The elongation remains at a higher percentage of 29.24%, which will help to avoid rupture during sudden acceleration and exhaust forces. Even though C3 has good density, the higher needle punching and number of glass fibres penetrating the ceramic surfaces act

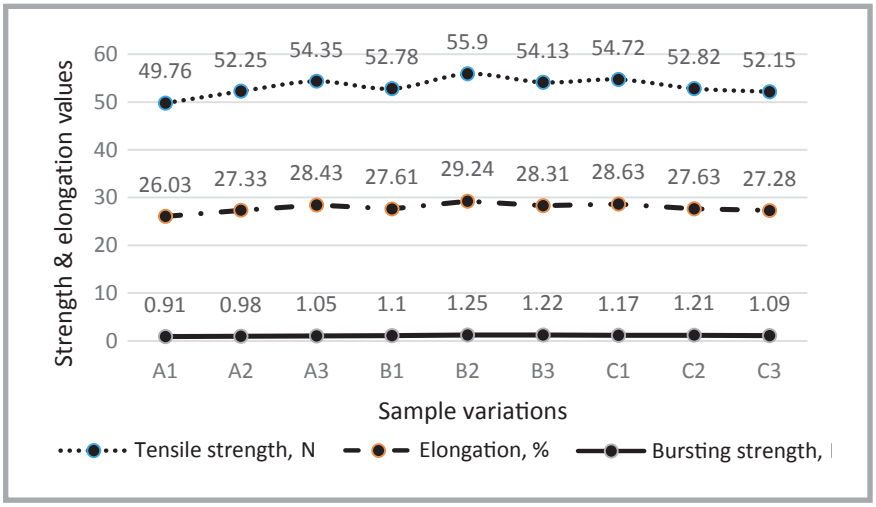

Figure 7. *Effect of needle punching and materials on strength and elongation properties.*

Table 3. *Mechanical properties of the composite materials.*

Sample code	Thickness, mm	Density, kg/m^3	Tensile strength, N	Elongation, %	Bursting strength, MPa
A1	3.56	187.38	49.76	26.03	0.912
A2	3.13	204.87	52.25	27.33	0.981
A3	3.27	205.18	54.35	28.43	1.049
B1	3.22	220.50	52.78	27.61	1.098
B2	2.53	275.50	55.90	29.24	1.245
B3	2.95	251.30	54.13	28.31	1.216
C1	2.94	254.90	54.72	28.63	1.167
C2	2.49	296.70	52.82	27.63	1.206
C3	2.90	259.90	52.15	27.28	1.089

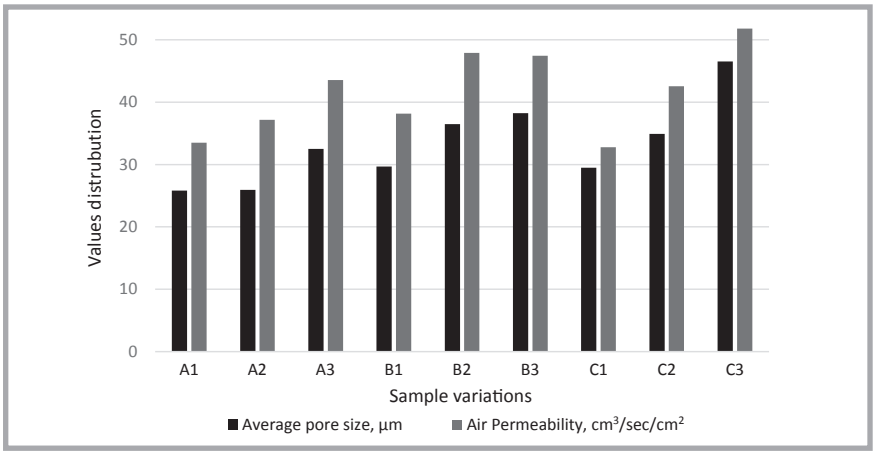

Figure 8. *Surface properties of composite materials.*

Table 4. *Thermal properties of flexible composite samples.*

Sample code	Thermal conductivity, W/(m·K)	Thermal resistance, m^2 KW	Thermal transmittance, W/(m^2 K)	Thermal diffusivity ×10^7, m^2/s
A1	0.0306	0.1162	8.604	1.66
A2	0.0321	0.0974	10.263	1.59
A3	0.0318	0.1028	9.728	1.57
B1	0.0305	0.1056	9.468	1.40
B2	0.0310	0.0816	12.248	1.14
B3	0.0324	0.0912	10.969	1.30
C1	0.0322	0.0914	10.938	1.28
C2	0.0312	0.0797	12.542	1.07
C3	0.0314	0.0923	10.839	1.23

as a reversal process of the reduction of strength.

Effect on surface properties

The porosity of the composites and the permeability brings a very narrow variation and almost forms a parallel distribution. Although the porosity results of the samples show in the pore sizes; addition to that, for the flexible composites the permeability also verified and given in ***Figure 8***. Based on the results, optimum results were identified in four readings as A3, B2, C1 and C2, nearing the average values both in the porosity and permeability. Based on the mechanical parameters, A3, B2 and C2 show a reduction in mechanical characteristics, B2 can be taken for consideration. Sample C3 shows a very good porosity of 46.50 µm and permeability of 51.78 $cm^3/s/cm^2$, which is due to the higher punches per unit area in the nonwoven, making the glass fibres open in the ceramic fibre layers instead of interlocking.

Effect on thermal properties

As mentioned above [3], the constitutive material should have a good thermal conduction property. ***Table 4*** shows the thermal properties of the samples of flexible composites. Material C1 shows a good thermal conductivity, while B1 is lower. Meanwhile the resistivity of the samples for the filter wall shows a higher value for sample B3 due to the varying thickness and density; hence the sample is not considered. B2 shows an average thermal conductivity of 0.310 W/(m K) but lower resistivity of 0.0816 m^2 KW, which is due to its lower thickness, and hence B2 may be considered for its better thermal conduction property and filtration performance. Subsequently B2 shows a higher thermal transmittance value of 12.25 W/(m^2 K), which will help in higher heat transfer from the filter surface. At the same time, the thermal diffusivity shows a reversal process, where the minimal value for B2 is 1.14×10^{-7} m^2/s, upon which density has an effect. This result shows that B2 will be a better option for the good conduction of heat with a slow diffusion rate, which can maintain a temperature of the walls around a maximum of 550 °C, where the regeneration process can occur to burn unburnt soot particles [19, 20].

Thermal expansion

The material is subjected to a continuous process of heat flow of around 400-500 °C inside the exhaust system, hence there will be heating and cooling of the media in the process. The thermal expansion during the heating of the material expressed the monotonic increasing relationship between the temperature and length of the material [1]. Eventually the coefficient of thermal expansion of the Ceramic (SiC) presents a range of 4.7-5.2 10^{-6} K^{-1} [21] and for E-Glass fibres: 4.9-6.0 10^{-6} K^{-1} [22], respectively. Although they show very weak expansion over the temperature range up to 800 °C, the test may not be considered for further analysis, where the internal application requirement is at the maximum up to 600 °C.

Statistical evaluation

Considering the two factors of the needling density in punches/cm^2 and weight of the composite in g/m^2, the two factors without replication model ANOVA test is performed (***Table 6***). Each response is compared with 09 samples and the p value noted. The value of p less than 0.05 indicates all the responses have significant effects at a 95% confidence level.

The properties of thickness and densities show a p value < 0.05, which are significant. GSM and the needling densities have a major effect on the differences in material performance for these properties. As mentioned earlier, with a lower thickness and higher bulk densities, sample B2 will be a better selection among the samples.

Statistical evaluation of mechanical properties shows that the tensile strength and elongation at break properties are not significant (Tensile p = 0.49002, Elongation p = 0.73006) neither for the GSM nor the needling density. And the strength majorly depends upon the sewing of the composite layers with

Table 6. *Statistical data. GSM – grams per square metre, S – significant, NS – not significant.*

Response	Source of variation	Sum of squares	Degrees of freedom	Mean square	F value	P value	F Critical	Result
Thickness	GSM	0.4868	2	0.243	22.31	0.00677	6.944	S
	Needling density	0.4184		0.209	19.17	0.00892		S
Density	GSM	8046		4022	27.29	0.00466		S
	Needling density	2180		1090	7.394	0.04432		S
Tensile strength	GSM	0.07219		0.0361	0.8571	0.49002		NS
	Needling density	0.02915		0.0146	0.3461	0.72670		NS
Elongation at break	GSM	1.894		0.947	0.8515	0.49193		NS
	Needling density	0.7578		0.378	0.3407	0.73006		NS
Bursting strength	GSM	7.642		3.821	8.470	0.03649		S
	Needling density	1.182		0.591	1.310	0.36502		NS
Porosity	GSM	128.6		64.32	5.745	0.06669		NS
	Needling density	176.1		88.05	7.863	0.04112		S
Air permeability	GSM	64.45		32.22	2.915	0.16556		NS
	Needling density	248.1		124.0	11.22	0.02288		S
Thermal conductivity	GSM	1.40E-07		70E-08	0.09745	0.90924		NS
	Needling density	8.87E-07		4.43E-07	0.6172	0.58398		NS
Thermal resistance	GSM	0.0004976		0.0002488	11.99	0.02043		S
	Needling density	0.0004951		0.0002475	11.93	0.02061		S
Thermal transmittance	GSM	5.797		2.898	11.68	0.02137		S
	Needling density	6.140		3.070	12.37	0.01937		S
Thermal diffusivity	GSM	2.83E-15		1.42E-15	39.25	0.00235		S
	Needling density	4.90E-16		2.45E-16	6.778	0.05191		S

filament yarn in uniform intervals. While the bursting strength, even though it depends upon the tensile and elongation behaviours of the textile material, based on the GSM, shows to be significant ($p = 0.03649$). Consequently, due to the larger fibre entanglements in the bulk thickness, although bursting is a force applied in expanding the material multi-directionally, the support of the thickness helps to perform in a positive manner. In the case of needle punching, the number of punches is not significant at all, where the p value is 0.36502. Similar to the tensile force, the stitch density applied on the material will overcome the performance in the testing. Frim the evaluation process, sample B2's result is the most satisfactory among the 9 samples, showing a higher strength and elongation.

The porosity and air permeability analysis with respect to the GSM factor does not show any significant changes, but variation did occur due to the needling factor ($p = 0.04112$ for porosity and $p = 0.02288$ for air permeability), as needling makes more punches, leading to a significant variation in the samples. As discussed earlier, sample B2 shows a good permeable property along with porosity for better filtration and maintenance of proper pressure management inside the exhaust media.

In the evaluation of thermal properties, the samples did not show any significance for GSM ($p = 0.90924$) and needling densities ($p = 0.58398$), which defines them as an insulator. The shape of fibres and their surface area will not influence the thermal conductivity more [23]. But due to the voids available in the samples and the thickness and densities as well as other permeable properties, the expected better thermal conductivity of the material is based purely on the test results. Among the samples, along with other properties to be taken into consideration. However, thermal properties like resistance, transmittance and diffusivity were significantly affected by GSM – needling density factors. These factors will support sample B2 in particular, where better thermal conductivity along with low resistance slow diffusivity and transmittance, which can be used for better performance in the study of filtration s.

Conclusions

New types of samples with ceramic and glass flexible nonwoven composites were made and analysed for their structural, surface, mechanical and thermal properties. Considering the filter media properties expected, such as low thickness and high density requirements, sample B2 suits the criteria. On account of the requirement of higher tensile, elongation and bursting properties which are essential for the filter walls, higher pressure comes out of the exhaust systems. Sample B2 meets these properties the most among the samples.

On the other hand, when thermal conductivity is more essential, sample B3 has the best performance. Furthermore for the subsequent thermal performances i.e. thermal resistance, transmittance and diffusivity, again B2 reacts well among the samples, which approaches the original DPF walls, with the thermal conductivity also being similar. Thus it is concluded that sample B2 (non-woven sample of ceramic glass of 200 g/m^2 with 300 g/m^2 of glass fibre with 100 punches/cm^2 in needling) will be taken into consideration for further research work to construct Particulate Matter Filters. This conclusion shows that the lower density of glass fibres in the sample a makes less binding with ceramic fibres at needling densities of either 75, 100 and 125 and that higher density of glass fibre makes lesser binding at a 75 needling density and opening up of the nonwoven at 100 and 125 needling densities.

References

1. Lee SJ, Jeong SJ, Kim WS. Numerical design of the diesel particulate filter for optimum thermal performances during regeneration. *Applied Energy* 2009; 86: 1124-1135.
2. Frank B, Schlogl R, Su DS. Diesel soot toxification. *Environmental Science Technololgy* 2013; 47: 3026-3027.
3. Benaqqa C, Gomina M, Beurotte A, Boussuge M, Delattre B, Pajot K, Pawlak E, Rodrigues F. Morphology, physical, thermal and mechanical properties of the constitutive materials of diesel particulate filters. *Applied Thermal Engineering* 2014; 62: 599-606.
4. Tsuneyoshi K, Hayama S. A new SiC-based DPF for the Automotive Industry. In: *DEER Conference*, 6 August 2008, pp. 1-14 Corporation, Dearborn, Michigan.
5. Stamatellou AM, Stamatelos A. Overview of Diesel particulate filter systems sizing approaches. *Applied Thermal Engineering* 2017; 121: 537-546.
6. Bueno-López A. Diesel soot combustion ceria catalysts. *Applied Catalysis B Environmental* 2014; 146: 1-11.
7. Burch R. Knowledge and know-how in emission control for mobile applications. *Catalysis Review* 2004; 46: 271-334.
8. ASTM D1777-96: 2015. Standard Test Method for Thickness of Textile Materials, ASTM International, West Conshohocken, PA.
9. Jaksic D, Jaksic N. Porosity of the flat textiles. Woven Fabric Engineering, Sciyo: 2010, pp. 255-272.
10. BS 5636: 1990. Method of test for the determination of the permeability of fabrics to air, British Standards, London, England.
11. ASTM D5035-11: 2015. Standard Test Method for Breaking Force and Elongation of Textile Fabrics (Strip Method), ASTM International, West Conshohocken, PA.
12. ASTM D3786/D3786M-18: 2018. Standard Test Method for Bursting Strength of Textile Fabrics – Diaphragm Bursting Strength Tester Method, ASTM International, West Conshohocken, PA.
13. Lee C. Heat transfer of fibrous insulation battings. Army Natick Research and Development Command technical report/ TR-84/055, USA, May 1984.
14. Gibson PW, Lee C, Frank K. Application of nano fiber technology to nonwoven thermal insulation. *Journal of Engineered Fibers and Fabrics* 2007; 2: 32-40.
15. Zakriya GM, Ramakrishnan G, Palani Rajan T, Abinaya D. Study of thermal properties of jute and hollow conjugated polyester fibre reinforced non-woven composite. *Journal of Industrail Textiles* 2017; 46: 1393-1411.
16. Mahmood N, Yuan Z, Schmidt J, Xu CC. Depolymerization of lignins and their applications for the preparation of polyols and rigid polyurethane foams: A review. *Renewable and Sustainable Energy Reviews* 2004; 60: 317-329.
17. BS 6993: 1989. Thermal and radiometric properties of glazing. Part 1: method of calculation of steady state U value.
18. Dos Santos WN, Mummery P, Wallwork A. Thermal diffusivity of polymers by the laser flash technique. *Polymer Testing* 2005; 24: 628-634.
19. Konstandopoulos AG, Kostoglou M, Skaperdas E, Papaioannou E, Zarvalis D, Kladopoulou E. Fundamental studies of diesel particulate filters: transient loading, regeneration and aging. *SAE paper* 2000; 1: 1016-1023.
20. Deuschle T, Janoske U, Piesche M. A CFD-model describing filtration, regeneration and deposit rearrangement effects in gas filter systems. *Chemical Engineering Journal* 2008; 135: 49-55.
21. Adler J. Ceramic diesel particulate filters. *International Journal of Applied Ceramic Technology* 2005; 2: 429-439.
22. Sakka S, Kamiya K. The sol-gel transition in the hydrolysis of metal alkoxides in relation to the formation of glass fibers and films. *Journal of Non Crystalline Solids* 1982; 48: 31-46.
23. Martin JR, Lamb GE. Measurement of thermal conductivity of nonwovens using a dynamic method. *Textile Research Journal* 1987; 57: 721-727.

Received 14.06.2018 Reviewed 04.12.2018